Groundwater

Modeling the Effects of Naturally Occurring Organic Carbon on Chlorinated Ethene Transport to a Public Supply Well†

by Francis H. Chapelle[1], Leon J. Kauffman[2], and Mark A. Widdowson[3]

Abstract

The vulnerability of public supply wells to chlorinated ethene (CE) contamination in part depends on the availability of naturally occurring organic carbon to consume dissolved oxygen (DO) and initiate reductive dechlorination. This was quantified by building a mass balance model of the Kirkwood-Cohansey aquifer, which is widely used for public water supply in New Jersey. This model was built by telescoping a calibrated regional three-dimensional (3D) MODFLOW model to the approximate capture zone of a single public supply well that has a history of CE contamination. This local model was then used to compute a mass balance between dissolved organic carbon (DOC), particulate organic carbon (POC), and adsorbed organic carbon (AOC) that act as electron donors and DO, CEs, ferric iron, and sulfate that act as electron acceptors (EAs) using the Sequential Electron Acceptor Model in three dimensions (SEAM3D) code. SEAM3D was constrained by varying concentrations of DO and DOC entering the aquifer via recharge, varying the bioavailable fraction of POC in aquifer sediments, and comparing observed and simulated vertical concentration profiles of DO and DOC. This procedure suggests that approximately 15% of the POC present in aquifer materials is readily bioavailable. Model simulations indicate that transport of perchloroethene (PCE) and its daughter products trichloroethene (TCE), *cis*-dichloroethene (*cis*-DCE), and vinyl chloride (VC) to the public supply well is highly sensitive to the assumed bioavailable fraction of POC, concentrations of DO entering the aquifer with recharge, and the position of simulated PCE source areas in the flow field. The results are less sensitive to assumed concentrations of DOC in aquifer recharge. The mass balance approach used in this study also indicates that hydrodynamic processes such as advective mixing, dispersion, and sorption account for a significant amount of the observed natural attenuation in this system.

Introduction

Chlorinated ethenes (CEs) are among the most common volatile organic compounds (VOCs) observed to contaminate public supply wells in the United States (Zogorski et al. 2006). The vulnerability (V) of public supply wells to CE contamination is a complex function of the intrinsic susceptibility (IS) of a given aquifer, chemical mobility and persistence (CMP), and chemical inputs (CI) to a system as illustrated by the generalized equation (Focazio et al. 2002):

$$V = f\,(\mathrm{IS}, \mathrm{CMP}, \mathrm{CI})\,. \qquad (1)$$

IS refers to the physical properties of an aquifer such as the distribution of hydraulic conductivity and the distribution and amounts of recharge. Contaminant mobility and persistence depends partly on the chemical properties of individual contaminants, and also on the geochemical conditions encountered in different aquifers (Feinstein and Thomas 2008). This is particularly important for CEs that are subject to microbial reductive dechlorination processes that can be driven by naturally occurring sources of dissolved organic carbon (DOC) and particulate organic carbon (POC) (U.S. EPA 1998; Bradley 2003; Rectanus

[1]Corresponding author: U.S. Geological Survey, South Carolina Water Science Center, Columbia, SC 29210; (803) 750-6116; fax: (803) 750-6181; chapelle@usgs.gov

[2]U.S. Geological Survey, Montana Water Science Center, Bozeman, MT, 59601.

[3]Via Department of Civil and Environmental Engineering, Virginia Tech, Blacksburg, VA, 24061.

†Prepared for the National Water Quality Assessment (NAWQA) and the Toxics Substances Hydrology Programs of the U.S. Geological Survey.

Received July 2013, accepted November 2013.

doi: 10.1111/gwat.12152

et al. 2007). It has long been observed that aquifers containing little natural organic carbon tend to have oxic conditions that inhibit reductive dechlorination, whereas aquifers containing more abundant natural organic carbon tend to be anoxic and support efficient reductive dechlorination (Wiedemeier et al. 1999; Chapelle et al. 2012). Building quantitative models that are based on a mass balance between electron donors such as organic carbon and electron acceptors (EAs) such as dissolved oxygen (DO), and CEs, however, is challenging (Feinstein and Thomas 2008). The purpose of this paper was to use a numerical mass balance modeling approach designed specifically to couple the interactions of organic carbon, DO, and CEs in order to more realistically simulate the fate and transport of CEs in groundwater systems.

The mass balance approach used in this paper is explicitly based on the definition of well vulnerability given in Equation 1. The first step is to accurately describe the IS of the aquifer, which is broadly interpreted as understanding the hydraulic conductivity distribution, sources of aquifer recharge and discharge, and the resulting directions and rates of groundwater flow. The second step is to couple the mobility and persistence of the concerned contaminant, which in this case is perchloroethene (PCE), with ambient reduction/oxidation (redox) conditions in the aquifer. PCE is subject to reductive dechlorination when concentrations of DO decrease below approximately 0.5 mg/L (Chapelle et al. 2012). Thus, in order to realistically simulate PCE transformation, it is necessary to consider the delivery, transport, and biological uptake of DO in the aquifer. The biological uptake of DO, in turn, is affected by the amount and bioavailability of organic carbon present in or being delivered to the aquifer. The third step is to describe the effects of CI of PCE on the aquifer. The efficiency of PCE transformation will depend on the length of individual flowpaths carrying PCE contaminants and the redox conditions encountered along these flowpaths. The length and redox conditions encountered, in turn, will be determined by the location of PCE sources within the three-dimensional (3D) flow field and the concentrations of those sources. Only when each term of Equation 1 is quantified, it is possible to construct a true mass balance for assessing the vulnerability of individual public water supply wells to PCE contamination.

Interactions of Organic Carbon, DO, and CEs

There are at least three distinct compartments in groundwater systems that store natural organic carbon, capable of reacting with DO, CEs, and other EAs. DOC is present at varying concentrations in all groundwater systems (Leenheer 1974; Thurman 1985; Aiken 1989), and this dissolved compartment can store significant amounts of organic carbon. In addition, many groundwater systems contain POC in various stages of diagenesis (Aiken 1989, Thurman 1985; McMahon et al. 1990; Lilienfein et al. 2004). Microbial degradation of POC can be an additional source of DOC to soil interstitial water (Kalbitz et al. 2000) and groundwater (McMahon and Chapelle 1991). Finally, silicate, iron oxyhydroxide, and other minerals present in aquifer solids have a significant capacity to adsorb DOC (Kahle et al. 2004), removing it from the dissolved phase (Davis 1982; Findlay and Sobczak 1996; Lilienfein et al. 2004; Jardine et al. 2004). These adsorption processes are partially reversible, so that desorption of organic carbon from aquifer materials is also a potential source of DOC (Gu et al. 1995). In addition to acting as sinks and sources of DOC, sorption processes can also fractionate DOC, irreversibly sorbing hydrophobic humic compounds while allowing subsequent desorption of more hydrophilic compounds (Oren and Chefetz 2012). A mass balance model of organic carbon dynamics in groundwater systems, therefore, will need to address each of these carbon-storing compartments and their interactions.

In contrast to the complexity inherent in the multiple sources, sinks, and composition of DOC, atmospheric oxygen carried through the unsaturated zone by infiltrating precipitation is the sole source of DO to groundwater systems, which lack active photosynthesis. In addition, DO's relatively limited solubility in fresh water (10.1 mg/L at 15 °C) provides a convenient upper limit to concentrations of DO that can be delivered to the water table. These characteristics will be useful in constraining a quantitative mass balance between DOC and DO.

The interaction of DO with the three compartments of organic carbon present in groundwater systems determines the transformation or lack of transformation of CEs. The usual ecological succession of EA use in groundwater systems (oxygen > CEs > Fe(III) > sulfate > carbon dioxide; McMahon and Chapelle 2008) implies that once concentrations of DO drop below approximately 0.5 mg/L, reduction of CEs will occur under any of the succeeding predominant terminal electron-accepting processes. Construction of a mass balance between the sources and bioavailability of DOC and DO, therefore, is central to assessing well vulnerability to CE contamination.

Methods

Study Area

The hydrologic system used to illustrate the interactions of natural organic carbon, DO, and CE contaminants is the Kirkwood-Cohansey aquifer in the vicinity of Glassboro, New Jersey. This aquifer is an important source of public water supply in southern New Jersey. Because much of this aquifer system is unconfined, it is relatively vulnerable to contaminants such as nitrate (Kauffman et al. 2001) and CEs (Zogorski et al. 2006). The study area (Figure 1) is underlain by coastal plain sediments of the Cohansey and Kirkwood Formations of the middle and early Miocene age, respectively (Owens and Minard 1979). The shallower Cohansey Formation sediments consist of white, yellow, or gray medium sands that contain discontinuous interbedded clays. The deeper Kirkwood Formation consists of fine-to-medium, white-to-pale gray sand. Its deepest sediments consist of dark lignitic

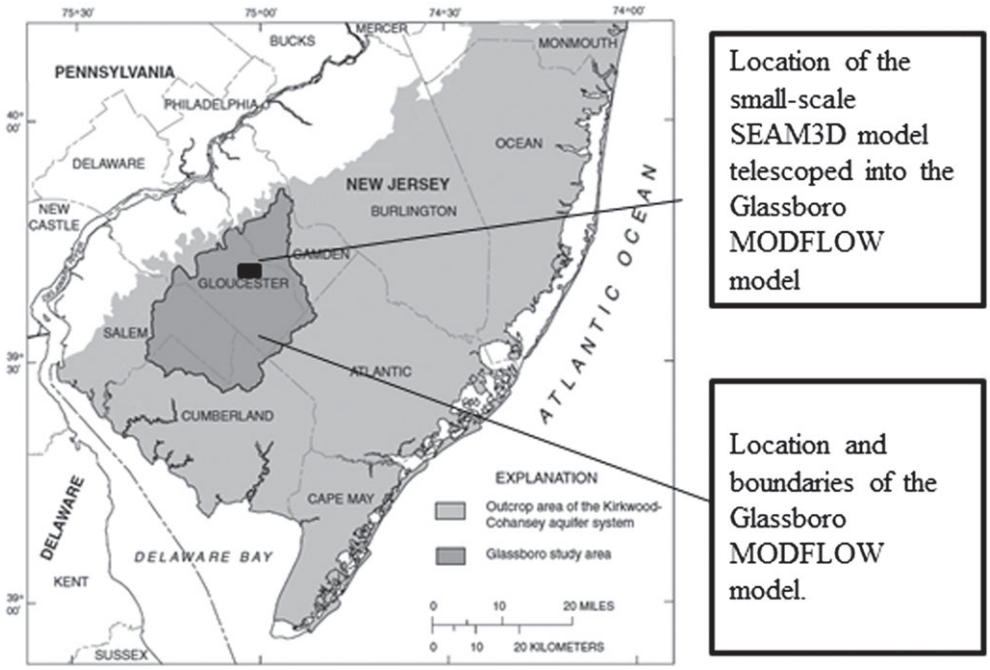

Figure 1. Map showing the boundaries of the Glassboro MODFLOW model and the location of the telescoped SEAM3D within the MODFLOW model.

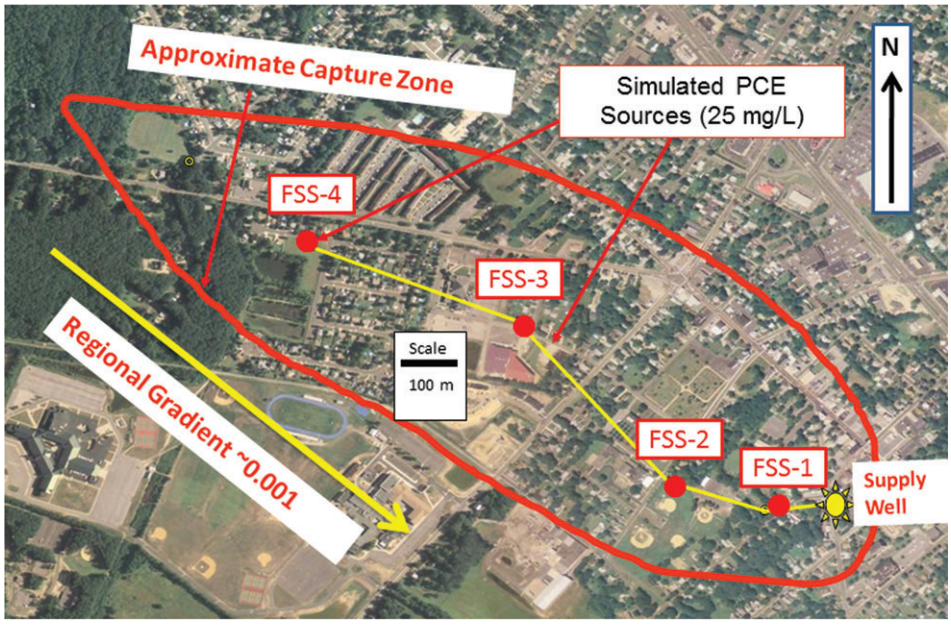

Figure 2. Location of the approximate capture zone of the public supply well, locations of the well clusters used for geologic and water chemistry control, and location of the two simulated contaminant source areas.

clays and silts. The locations of multilevel observation wells drilled for geologic, hydrologic, and geochemical control are shown in Figure 2. The approximate capture zone of the public supply well considered in this study is also shown in the figure. Note that the observation wells are approximately oriented along a flowpath leading to the public supply well. All water chemistry data used in this paper were collected by the National Water Quality Assessment (NAWQA) program of the U.S. Geological Survey (Zogorski et al. 2006).

The generalized lithology of the Kirkwood-Cohansey aquifer, as determined by drilling and electrical logs of the monitoring wells, is shown in cross section in Figure 3. The white or yellow sandy sediments contain relatively low amounts of organic carbon, with measured amounts of particulate and adsorbed organic sediments ranging from 0.1 to 0.3 weight percent (wt/%) (Table 1). By contrast, the discontinuous interbedded clays and silts contain more organic carbon, with measured amounts ranging up to 2.85 wt/% (Table 1). The sands of the

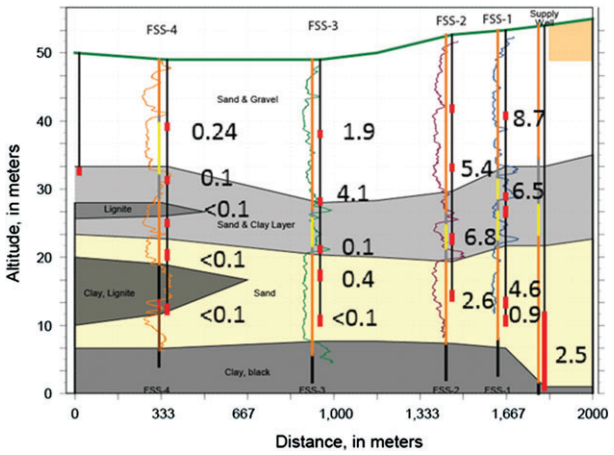

Figure 3. Geologic cross section illustrating the distribution of sands and clays along the flowpath leading to the public supply well and measured concentrations of DO (mg/L) with depth.

Table 1
Organic Carbon Content Measured in Cores of Aquifer Sediments

Well Number[1] (Figure 3)	Sample Depth (Meters Below Land Surface)	Sediment Texture	Organic Carbon Content (wt/%)
FSS1-3	27	Gray clay	2.06
FSS1-4	40	White sand	0.33
FSS2-2	30	White sand	0.15
FSS3-4	95	Yellow sand	0.28
FSS4-4	43	Black clay	2.85

[1]Well cluster locations shown in Figures 2 and 3.

Cohansey Formation were deposited unconformably on top of the Kirkwood sands, and the two geologic units function as a single aquifer system (Kauffman et al. 2001; Cauller and Carleton 2005).

The water chemistry of Kirkwood-Cohansey aquifer, as delineated by the multilevel monitoring wells (Figure 3), is strongly affected by the distribution of organic carbon in aquifer sediments and by pumping from the public supply well (Table 2). Concentrations of DO are highest at and near the public supply well (Figure 3), which reflects rapid transport of oxygen-bearing water from the top of the water table due to pumping. Concentrations of DO are lowest at the FSS4 well cluster, which penetrated relative organic-rich sediments (Figure 3) and is less affected by pumping from the supply well. Concentrations of dissolved iron were the highest whereas concentrations of DO were the lowest (Table 2), indicating an active Fe(III) reduction in parts of the aquifer. Similarly, concentrations of sulfate were lowest where DO concentrations were the lowest, indicating an active sulfate reduction in parts of the aquifer as well. DOC concentrations were generally lower than 1 mg/L. The highest concentrations of CE were found in water produced from the public supply well. PCE was present at the highest concentrations (~53 µg/L), and trichloroethene (TCE) and *cis*-dichloroethene (*cis*-DCE) were present at low but measurable concentrations (~1 µg/L). Vinyl chloride (VC) concentrations were below measurable concentrations in groundwater produced from all the wells. The observed concentrations of DO, DOC, and CEs provide a baseline for constraining the mass balance model.

MODFLOW Model of the Kirkwood–Cohansey Aquifer

The numerical model developed in this study is based on a model originally developed to investigate the effects of land use and groundwater travel times on nitrate concentrations in the study area (Kauffman et al. 2001). The USGS 3D finite-difference code MODFLOW-96 (Harbaugh and McDonald 1996) was used to simulate groundwater flow and water-level distributions across the study area (Figure 1). This regional model was constructed using a 3D grid consisting of 343 columns, 214 rows, and 12 layers. The 150 m × 150 m cells were uniform in dimension, and model layers varied from 6.1 m to 24 m in thickness. Locally, several hydrostratigraphic units (Kirkwood Formation, Cohansey Sand and Bridgeton Formation) function together as an unconfined aquifer system. Recharge is the primary input to the aquifer system with groundwater discharge primarily to streams and pumping wells. No-flow boundaries surround the external boundary of the regional model. Details of the model, including input parameters, calibration, flow budget, and travel times are described in Kauffman et al. (2001).

The regional flow model was calibrated by adjusting horizontal, vertical, and streambed hydraulic conductivities to achieve a match to observed groundwater levels. In addition, simulated base flows of streams in the study area were compared to measured base flows to further constrain the model. This model (Kauffman et al. 2001) was then updated using MODFLOW-2005 (Harbaugh 2005) and the hydraulic conductivity distribution was further refined by comparing observed and simulated groundwater age distributions.

The Sequential Electron Acceptor Model in 3D

The Sequential Electron Acceptor Model in 3D (SEAM3D) was used to construct a quantitative mass balance between electron donors and acceptors in this study (Waddill and Widdowson 1998). The code is designed to simulate the transport of reactive constituents including a range of redox-based biodegradation problems involving hydrocarbon and chlorinated compounds (Waddill and Widdowson 2000). SEAM3D consists of a base code (MT3DMS) for physical transport and a number of modules for aerobic and anaerobic biodegradation, NAPL dissolution, and reductive dechlorination of chlorinated VOCs. Both MODFLOW and SEAM3D were implemented using the Groundwater Modeling System (AQUAVEO™, Provo, Utah).

Because of the computational complexity of this mass balance, it was not feasible to model the entire area of the Kirkwood-Cohansey aquifer (Figure 1). Rather, a small-scale model (3 square miles; Figure 2) was

Table 2
Water Quality Parameters for Flowpath Wells Screened in the Kirkwood-Cohansey Aquifer

	Well Numbers (Figure 3)																		
Parameter	**FSS 1-1**	**FSS 1-2**	**FSS 1-3**	**FSS 1-4**	**FSS 1-5**	**FSS 2-1**	**FSS 2-2**	**FSS 2-3**	**FSS 3-1**	**FSS 3-2**	**FSS 3-3**	**FSS 3-4**	**FSS 3-5**	**FSS 4-1**	**FSS 4-2**	**FSS 4-3**	**FSS 4-4**	**FSS 4-5**	**Supply Well**
pH (units)	4.89	4.4	4.49	4.39	4.49	4.9	4.38	4.25	5.02	5	5.2	4.69	5.43	5.26	5.4	4.6	4.9	4.8	4.77
Specific Conductance ($\mu Si/cm^2$)	154.8	82.4	67.7	64.8	56.2	284.6	245.9	75.4	188.2	372.5	77.6	86.9	41.69	161.6	140.2	86.7	30.35	33.04	101
Temperature (°C)	16.1	16.5	17.1	16.19	15.66	16.8	17.4	17.1	18.2	17.6	17.2	17.2	16.7	17.4	18.6	17	16.7	16.5	14.2
Calcium	5.67	3.83	2.45	0.892	1.542	8.459	10.08	0.537	5.924	13.75	2.036	0.98	0.744	2.471	1.859	2.767	1.092	0.373	10.87
Magnesium	2.50	1.48	1.60	0.878	1.053	2.352	4.341	0.6	1.637	2.224	2.021	2.193	0.502	1.608	0.942	0.994	0.409	0.332	2.604
Potassium	3.86	1.30	1.29	1.213	1.195	2.399	3.451	1.87	2.327	3.409	1.178	1	0.919	2.728	0.943	0.908	0.522	0.905	0.753
Sodium	15.4	4.15	5.20	7.384	4.486	36.12	22.41	9.207	24.25	51.17	6.255	8.571	2.509	21.12	20.55	6.909	1.418	1.37	4.701
Alkalinity	na	na	na	na	na	5.8	7.8	na	3.9	5.05	3.95	na	4.95	4.5	9.4	na	na	1.5	8.6
Chloride	22.9	12.3	12.1	11.9	8.7	47.9	43.7	14.3	24.0	80.5	16.0	20.7	4.8	34.6	32.1	12.5	2.6	2.1	16.6
Sulfate	11.48	7.51	0.19	0.73	5.05	29.32	24.58	2.23	33.71	21.75	0.56	0.11	3.82	7.25	1.13	14.26	5.25	10.57	5.49
DO	8.68		6.47	4.56	0.86	5.4	6.8	2.59	1.92	4.1	0.1	0.4	0.49	0.24	0.1	< 0.1	< 0.1	0.3	2.5
Iron	0.012	0.086	0.015	0.014	0.067	0.023	0.009	0.037	0.060	0.041	0.93	0.085	3.33	0.34	0.58	0.59	1.08	1.97	0.013
Ammonia	< 0.01	< 0.01	< 0.01	< 0.01	< 0.01	0.018	< 0.01	0.010	< 0.01	0.013	0.027	< 0.01	0.018	0.206	0.016	< 0.01	< 0.01	0.017	0.112
Nitrate	2.75	0.91	1.49	1.56	0.569	2.937	2.751	1.168	0.716	2.997	0.821	0.385	0.026	0.075	< 0.02	< 0.02	< 0.02	< 0.02	2.54
DOC	0.92	0.36	0.26	4.48	0.29	0.84	0.67	0.49	0.57	0.51	0.30	0.27	0.27	0.54	0.64	0.34	0.51	0.62	0.37
PCE (µg/L)	< 0.03	< 0.03	< 0.03	< 0.03	< 0.03	0.249	0.093	< 0.03	0.049	0.097	< 0.03	< 0.03	< 0.03	< 0.03	< 0.03	< 0.03	< 0.03	< 0.03	53.66
TCE (µg/L)	< 0.03	< 0.03	< 0.03	< 0.03	< 0.03	< 0.03	< 0.03	< 0.03	< 0.03	< 0.03	< 0.03	< 0.03	< 0.03	< 0.03	< 0.03	< 0.03	< 0.03	< 0.03	1.04
cis-DCE (µg/L)	< 0.03	< 0.03	< 0.03	< 0.03	< 0.03	< 0.03	< 0.03	< 0.03	< 0.03	< 0.03	0.053	0.051	< 0.03	< 0.03	< 0.03	< 0.03	< 0.03	< 0.03	0.68
VC (µg/L)	< 0.03	< 0.03	< 0.03	< 0.03	< 0.03	< 0.03	< 0.03	< 0.03	< 0.03	< 0.03	< 0.03	< 0.03	< 0.03	< 0.03	< 0.03	< 0.03	< 0.03	< 0.03	< 0.03

Note: Units are expressed as mg/L unless otherwise noted.
na = not analyzed.

constructed that roughly encompasses the contributing area of a single public supply well. This public supply well has a history of contamination by CEs (Table 2). Because of the value of groundwater in southern New Jersey, however, the well remains active for use and the water is treated to remove CEs prior to distribution. The locations of multilevel monitoring wells approximately located along the flowpath of groundwater moving to the public supply wells that were used to collect geologic and geochemical data used to constrain SEAM3D are also shown in Figure 2.

The local model domain (Figure 1) consisted of 28 columns, 48 rows, and 9 model layers that used an identical model-layering system as the regional model, but a finer uniform numerical mesh (75 m × 75 m) was selected for the flow and simulation of transportation. The lateral boundaries were primarily specified head cells upgradient and downgradient of the pumping well, and where applicable, no-flow boundary conditions along the edge of the model domain corresponding with the regional horizontal groundwater flow. Both the regional and the local groundwater flow models were simulated under steady-state conditions using the average annual pumping rate for the public supply well. Simulated water levels in the local groundwater flow model were compared to the results of the calibrated regional model and verified to match the results of the larger model.

The use of the SEAM3D code requires specification of a large number of hydrodynamic, microbiological, Monod kinetic parameters and CE transformation parameters. The parameters used to simulate the Cohansey-Kirkwood model described in this paper were derived from an earlier application of the SEAM3D code to simulate a CE plume in a coastal plain aquifer in Georgia (Chapelle et al. 2007). The hydrologic conditions of the two aquifers—unconfined sandy water table aquifers underlain by organic-rich confining beds—are similar and PCE is the source contaminant in both systems. Chapelle et al. 2007 includes a detailed list of the hydrodynamic, microbiological, and Monod kinetic parameters used in the model described in this paper. The hydrologic and dispersion parameters used in the SEAM3D are summarized in Table 3.

Equations for the mass balance of bioavailable organic carbon and EAs assume that DOC serves as the primary electron donor (carbon/energy source) for a heterotrophic microbial population in the aquifer system. Physical and biogeochemical processes incorporated in equations of transport include advection, dispersion, microbially mediated biotransformation, rate-limited sorption, and desorption. For example, the mass balance equation for bioavailable DOC is given as

$$-\frac{\partial}{\partial x_i}\left(v_i C_{\mathrm{DOC}}\right)+\frac{\partial}{\partial x_i}\left(D_{ij}\frac{\partial C_{\mathrm{DOC}}}{\partial x_j}\right)+\frac{q_s}{\theta}C^*_{\mathrm{DOC}} - R^{\mathrm{bio}}_{\sin k,\mathrm{DOC}}-\rho_{\mathrm{b}}\frac{\partial \overline{C}_{\mathrm{DOC}}}{\partial t}=\frac{\partial C_{\mathrm{DOC}}}{\partial t}, \tag{2}$$

where $\overline{C}_{\mathrm{DOC}}$ is the concentration of bioavailable DOC in the solid phase [M/L^3]; C_{DOC} is the concentration of bioavailable DOC in the aqueous phase [M/M^3]; ρ_{b} is the bulk density of the subsurface material [M/L^3]; v_i is the average pore water velocity [L/T]; D_{ij} is the tensor for the hydrodynamic dispersion coefficient [L^2/T]; $R^{\mathrm{bio}}_{\sin k,\mathrm{DOC}}$ is a biodegradation sink term dependent on the mode of respiration [M/L^3/T]; C^*_{DOC} is the DOC concentration of the source or sink flux [M/L^3]; θ is aquifer porosity [–]; x_{ij} is distance along the respective Cartesian coordinate axis [L]; t is time [T]; and q_s is the volume flow rate per unit volume of aquifer representing fluid sources (positive) and sinks (negative) [1/T].

Mass balance equations of the aqueous phase EAs (DO and sulfate, respectively) are

$$-\frac{\partial}{\partial x_i}\left(v_i E_{\mathrm{O_2}}\right)+\frac{\partial}{\partial x_i}\left(D_{ij}\frac{\partial E_{\mathrm{O_2}}}{\partial x_j}\right)+\frac{q_s}{\theta}E^*_{\mathrm{O_2}} - R^{\mathrm{bio}}_{\sin k,\mathrm{O_2}}=\frac{\partial E_{\mathrm{O_2}}}{\partial t}, \tag{3A}$$

$$-\frac{\partial}{\partial x_i}\left(v_i E_{\mathrm{SO_4}}\right)+\frac{\partial}{\partial x_i}\left(D_{ij}\frac{\partial E_{\mathrm{SO_4}}}{\partial x_j}\right)+\frac{q_s}{\theta}E^*_{\mathrm{SO_4}} - R^{\mathrm{bio}}_{\sin k,\mathrm{SO_4}}=\frac{\partial E_{\mathrm{SO_4}}}{\partial t}, \tag{3B}$$

where $E_{\mathrm{O_2}}$ and $E_{\mathrm{SO_4}}$ are the aqueous phase concentrations [M/L^3] of DO and sulfate, respectively; $E^*_{\mathrm{O_2}}$ and $E^*_{\mathrm{SO_4}}$ are the DO and sulfate concentrations [M/L^3] of source or sink fluxes, respectively; and $R^{\mathrm{bio}}_{\sin k,\mathrm{O_2}}$ and $R^{\mathrm{bio}}_{\sin k,\mathrm{SO_4}}$ are the EA biodegradation sink terms [M/L^3/T^1], respectively. The consumption of the bioavailable Fe(III) concentration [M/M^3] in the solid phase, $\overline{E}_{\mathrm{Fe}}$, is expressed as

$$-R^{\mathrm{bio}}_{\sin\ k,\mathrm{Fe}}=\frac{\mathrm{d}\overline{E}_{\mathrm{Fe}}}{\mathrm{d}t}. \tag{4}$$

Biodegradation of DOC is a function of EA availability and is described using modified Monod kinetics (Waddill and Widdowson 1998). In summary, the overall approach is to write an equation of mass balance for each individual solute and solid-phase constituent considered

Table 3
Hydrologic and Dispersion Parameters Used in SEAM3D

Model Parameter	Model Input
Hydraulic conductivity (m/d)	0.073 to 155
Porosity (dimensionless)	0.3
Longitudinal dispersivity (m)	5.0
Transverse horizontal dispersivity (m)	0.5
Transverse vertical dispersivity (m)	0.04
Molecular diffusion coefficient (m^2/d)	5.0×10^{-5}

and then to solve these equations simultaneously in order to compute a true mass balance as a function of time and space.

Modeling Organic Carbon Dynamics in Groundwater Systems

The soil science literature has extensively studied the dynamics of DOC formation and transport in soils (review by Kalbitz et al. 2000), and this literature is a useful starting point for considering DOC dynamics in groundwater systems. The standard conceptual model of DOC dynamics in soils (Kalbitz et al. 2000) considers that the total amount of carbon present at any given time and place reflects DOC and POC delivery from surface sources, production of DOC from bioavailable POC, biodegradation of DOC and POC, and the adsorption/desorption of DOC on soil particles.

DOC mobilized from surface soils or sediments are one source of bioavailable DOC to groundwater, but DOC can also be generated from POC present in aquifer material as well (Feinstein and Thomas 2008). Of the total POC (POC_{tot}) present in an aquifer, only some fraction of it (POC_{bio}) is available to support microbial metabolism:

$$POC_{bio} = f POC_{tot}, \tag{5}$$

where f is the fraction of bioavailable POC. Microbial metabolism of POC_{bio} can generate additional DOC, and this process can be conceived of as a mass transfer from the particulate to the dissolved phase according to the equation:

$$\rho_b \frac{\partial \overline{C}_{DOC}}{\partial t} = -k_{DOC}\left(C^{eq}_{DOC} - C_{DOC}\right), \tag{6}$$

where k_{DOC} is the rate constant for DOC production [1/T] and C^{eq}_{DOC} is the aqueous concentration of DOC in equilibrium with POC at any point in the system [M/L^3]. The sorption-desorption of DOC onto aquifer materials such as silicate minerals, ferric oxyhydroxides, and POC has been observed to be quasi-linear (Oren and Chefetz 2012) and can be approximated using a simple linear isotherm:

$$\overline{C}_{DOC} = K_d C^{eq}_{DOC}, \tag{7}$$

where $\overline{C}_{DOC}$ is the concentration of DOC adsorbed to aquifer material and K_d is the distribution coefficient [L^3/M]. It is recognized, however, that this approximation is a simplification of sorption-desorption dynamics in sediments. Once the fraction (f) of bioavailable POC_{tot} is specified, the numerical model used in this paper uses Equations 2. through 7 to iteratively calculate concentrations of bioavailable DOC and POC in the system as a function of time and space. This bioavailable DOC then drives the sequential use of EAs such as DO, CEs, Fe(III), sulfate, and carbon dioxide. Note that this approach yields a closed mass balance, as envisioned by the model of Kalbitz et al. (2000), for the total amount of organic carbon stored in all three compartments as a function of time.

Mass Balance of CEs

Equations of mass balance for chlorinated ethenes (CEs) in the aqueous phase are developed assuming microbially mediated reductive dechlorination is the primary mechanisms for the reduction of higher molecular weight CEs to lower molecular weight CEs. In this case, tetrachloroethene (PCE) is the source of chloroethene contamination. The fate and transport of chlorinated ethenes are described by equations for PCE ($i = 1$), TCE ($i = 2$), DCE, ($i = 3$), and VC ($i = 4$), respectively:

$$-\frac{\partial}{\partial x_i}\left(v_i C_{CE_1}\right) + \frac{\partial}{\partial x_i}\left(D_{ij}\frac{\partial C_{CE_1}}{\partial x_j}\right) + \frac{q_s}{\theta}C^*_{CE_1} - R^{bio}_{sink,CE_1} = R_{CE_1}\frac{\partial C_{CE_1}}{\partial t}, \tag{8A}$$

$$-\frac{\partial}{\partial x_i}\left(v_i C_{CE_2}\right) + \frac{\partial}{\partial x_i}\left(D_{ij}\frac{\partial C_{CE_2}}{\partial x_j}\right) + \frac{q_s}{\theta}C^*_{CE_2} - R^{bio}_{sink,CE_2} + R^{bio}_{source,CE_2} = R_{CE_2}\frac{\partial C_{CE_2}}{\partial t}, \tag{8B}$$

$$-\frac{\partial}{\partial x_i}\left(v_i C_{CE_3}\right) + \frac{\partial}{\partial x_i}\left(D_{ij}\frac{\partial C_{CE_3}}{\partial x_j}\right) + \frac{q_s}{\theta}C^*_{CE_3} - R^{bio}_{sink,CE_3} + R^{bio}_{source,CE_3} = R_{CE_3}\frac{\partial C_{CE_3}}{\partial t}, \tag{8C}$$

$$-\frac{\partial}{\partial x_i}\left(v_i C_{CE_4}\right) + \frac{\partial}{\partial x_i}\left(D_{ij}\frac{\partial C_{CE_4}}{\partial x_j}\right) + \frac{q_s}{\theta}C^*_{CE_4} - R^{bio}_{sink,CE_4} + R^{bio}_{source,CE_4} = R_{CE_4}\frac{\partial C_{CE_4}}{\partial t}, \tag{8D}$$

where C_{CE_i} is the chlorinated ethene concentration [M/L^3]; $C^*_{CE_i}$ is the chlorinated ethene concentration [M/L^3] of source or sink fluxes; R_{CE_i} is a retardation factor [−] to account for equilibrium sorption of chlorinated ethenes $i = 1$ to 4; R^{bio}_{sink,CE_i} is a sink term [M/L^3/T] to account for the microbially mediated reduction of chlorinated ethenes $i = 1$ to 4; and R^{bio}_{source,CE_i} is a source term [M/L^3/T] to account for the production of reductive dechlorination daughter products, chlorinated ethenes $i = 2$ to 4. The rates of reduction in chlorinated ethene and production of reductive dechlorination daughter product are coupled to the EA concentrations. These expressions are described in detail in Widdowson (2004).

Simulation of CE Source Areas

A large component of the vulnerability of public supply wells to CE contamination depends on the location and concentration of contaminant source areas located within the well capture zone (Focazio et al. 2002; Frind et al. 2006). In 1950, the Glassboro area of southern

New Jersey was largely rural, with less than 10% of the land use being classified as urban. By the year 2000, however, urban land uses had increased to more than 25% of the landscape. The increasingly urban nature of the study area resulted in increasing exposure to a variety of VOCs including petroleum hydrocarbons and CEs. This has resulted in increasing detections of VOCs measured in public supply and monitoring wells. In the Long Island-New Jersey study unit of the National Water Quality Assessment (NAWQA) program of the U.S. Geological Survey, which includes the Glassboro study area, as many as 60% of the wells sampled had detections of VOCs above the 0.2 µg/L reporting limit (Zogorski et al. 2006).

In the Glassboro study area, however, the locations and concentrations of VOC source areas are unknown. In view of this, the approach taken in this study was to simulate two hypothetical source areas (Figure 2). The more proximal simulated source area is located near well cluster FSS3 (Figures 2 and 3) and assumes a constant PCE concentration of 25 mg/L. The location of the proximal source area was chosen because it simulates contaminants moving toward the public supply well under largely oxic conditions (Figure 3). The more distal simulated source area, which also assumes an initial PCE concentration of 25 mg/L, is located near well cluster FSS4 (Figures 2 and 3). This distal source area simulates contaminants moving toward the public supply well first under initially anoxic conditions that shift to oxic conditions as the flowpath converges on the public supply well (Figure 3).

Results

Previous studies have clearly demonstrated the importance of naturally occurring organic carbon driving the reductive dechlorination and natural attenuation of CEs in groundwater systems (U.S. EPA 1998; Bradley 2003; Chapelle et al. 2012). However, it has not previously been feasible to couple the oxidation of naturally occurring DOC and POC coupled to CE reduction in order to model the vulnerability of public supply wells to contamination (Focazio et al. 2002; Frind et al. 2006). Formulating this problem as a mass balance between organic carbon and available EAs, and by considering the bioavailability of POC, provides a framework for accomplishing this. With this formulation, it is possible to investigate the sensitivity of CE transformation to (1) the bioavailability of POC in the aquifer, (2) the amount of DOC and DO entering the aquifer with recharge, (3) the location of simulated contaminant source areas, and (4) the redox conditions encountered along the flowpath to the public supply well from each source.

Simulation of DO Concentrations

The principal controls on concentrations of DO in the Kirkwood-Cohansey aquifer and other unconfined aquifers are the volume of recharge reaching the water table, concentrations of DOC and DO in aquifer recharge, and the amount and bioavailability of POC in the aquifer. The maximum amount of DO present in recharge water is limited to about 10 mg/L due to solubility constraints. Observed concentrations of DOC in the aquifer (Table 2) suggest that less than 1 mg/L of DOC is present in aquifer recharge. The amount of POC present in the system varies systematically with lithology, with low concentrations of POC present in sandy aquifer sediments (~0.2 wt/%) and higher concentrations in clayey confining bed sediments (~2.0 wt/%; Figure 3; Table 1). The most unknown, therefore, is the fraction of POC that is readily bioavailable. By varying the assumed fraction of bioavailable POC, it was found that the closest match to observed DO concentrations (Figure 3) was obtained by assigning a fraction of bioavailable POC to be 0.15. That value is consistent with previous studies on POC bioavailability (Chapelle et al. 2012; Thomas et al. 2013).

The simulated steady-state distribution of DO according to that assumption is shown in Figure 4A. The observed match between measured and simulated DO concentrations is shown in Figure 4B. The observed higher DO concentrations in the vicinity of the pumping public supply well (Figure 3) is reproduced by the model (Figure 4A) and reflects induced recharge of high-DO water near the public supply due to pumping.

Model Sensitivity to POC Bioavailability

The sensitivity of PCE, TCE, DCE, and VC transformation to the bioavailability of POC is illustrated in Figure 5. The simulated location of the contaminant source area was the proximal source near the Academy Street well cluster (Figure 2). If zero percent of the organic carbon present in the aquifer is assumed to be bioavailable (as might be the case with anthracite coal), DO concentrations remain high and the PCE remains untransformed along flowpaths between the contaminant source area to the public supply well (Figure 5A). Under these simulated oxic conditions, PCE moves from the simulated contaminant source areas and begins to arrive at the supply well after about 10 years. PCE concentrations continue to increase until plateauing at a concentration of about 80 µg/L. By contrast, concentrations of TCE (Figure 5B), *cis*-DCE (Figure 5C), and VC (Figure 5D) do not increase due to the lack of organic carbon-driven biotransformation. As the simulated bioavailable fraction of the POC increases to 0.1, DO is consumed with depth in the aquifer, more PCE is transformed, less PCE reaches the public supply well, and progressively more TCE, *cis*-DCE, and VC reaches the well. When the fraction of bioavailable POC is increased to 0.15, progressively more transformation of PCE occurs.

Model Sensitivity to DO and DOC Concentrations in Recharge

The model can also be used to show the sensitivity of contaminant transport to the amount of DO being delivered to the aquifer via recharge. Figure 6 shows the sensitivity CEs reaching the supply well assuming

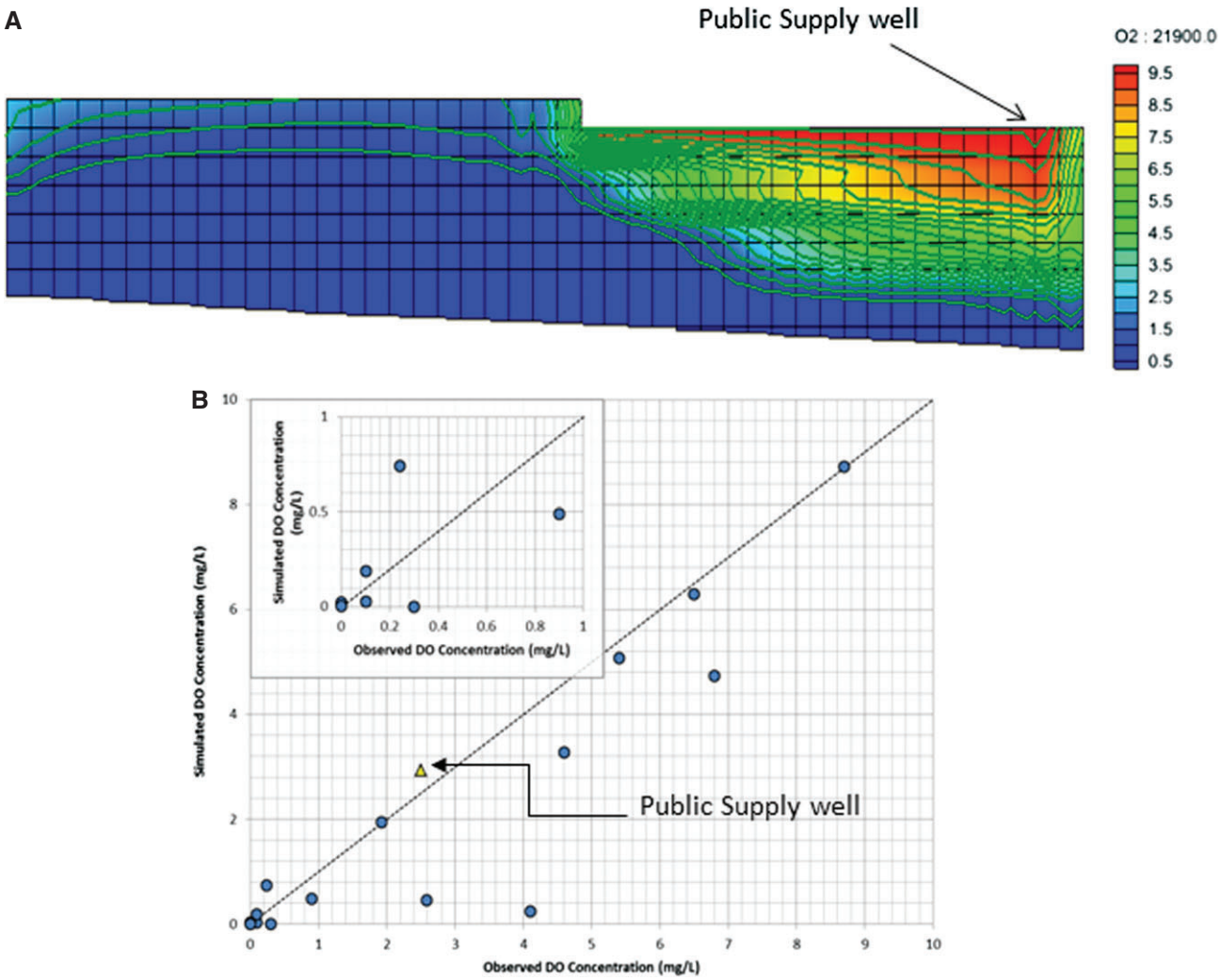

Figure 4. (A) Simulated concentrations of DO in a cross section ending at the public supply well assuming 15% bioavailable POC and (B) the match between measured and simulated concentrations of DO at steady state. The line shown is a 1:1 line. The least squares best fit line had a slope of 0.83 and an r^2 of 0.84.

that aquifer recharge has uniform DO concentrations of 10, 2, or 1 mg/L. The highest simulated concentration of PCE reaching the supply well occurs with the highest DO concentration (10 mg/L) in recharge (Figure 6A). Similarly, the lowest concentration of PCE reaching the supply well occurs with the lowest concentration of DO (1 mg/L) in recharge. Interestingly, however, the highest simulated TCE concentrations occur at the intermediate DO concentration (2.0 mg/L) (Figure 6B). This probably reflects interactions between the biological uptake of DO and the initiation of chlororespiration. The simulated behavior of *cis*-DCE mirrors the behavior of PCE (Figure 6C), with the highest *cis*-DCE concentrations reaching the supply well at the highest DO concentrations in recharge (Figure 6C). Concentrations of VC are extremely sensitive to DO concentrations in recharge (Figure 6D), with significant VC reaching the supply well only when assumed concentrations of DO in recharge are low (1 mg/L; Figure 6D).

While the simulation results are highly sensitive to concentrations of DO in recharge water, they are less sensitive to concentrations of DOC entering the aquifer in recharge water (Figure 7). Holding DO concentrations in recharge constant at 6 mg/L, and varying DOC concentrations in recharge water between 0.05, 0.2, and 1.5 mg/L, shows some difference in PCE concentrations reaching the supply well (Figure 7A). As expected, higher concentrations of DOC entering with recharge decreases concentrations of PCE reaching the public supply well. However, there was no observed difference in TCE concentrations reaching the supply well (Figure 7B). This lower sensitivity to DOC concentrations entering the aquifer with recharge reflects the interactions of the three different compartments that store organic carbon. As DOC enters the aquifer, it can be adsorbed if concentrations are higher than equilibrium with adsorbed DOC, or desorbed if DOC concentrations are lower than equilibrium. In addition, DOC can be generated from biodegradation of POC as well. The interaction of these carbon compartments has the effect of buffering the response of CE transformation to concentrations of DOC in recharge water.

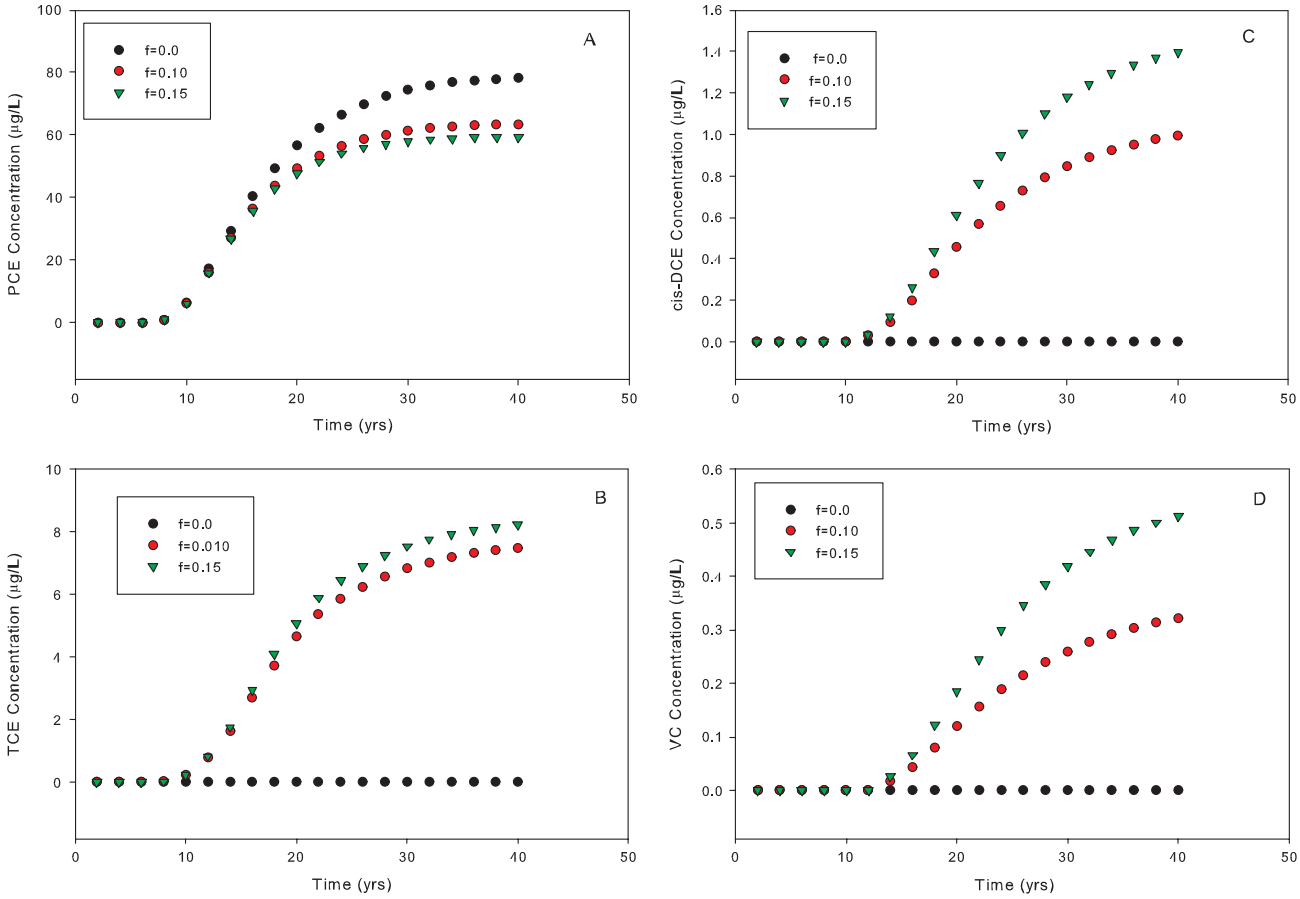

Figure 5. Simulated concentration changes of (A) PCE, (B) TCE, (C) *cis*-DCE, and (D) VC arriving at the public supply well as a function of time and the fraction of bioavailable POC present in the aquifer.

Model Sensitivity to Contaminant Source Area Location

The final variable in the generalized well vulnerability equation (Equation 1) is the location of contaminant source areas in relation to the flow system and the pumping well. The arrival of CE species from the proximal simulated source area located near well cluster FSS3 is shown in Figure 5. These simulations show CEs arriving at the supply well about 10 years following the release of contaminants to the aquifer. Assuming a bioavailable fraction of POC to be 0.15, the case that best reproduces the observed DO profile (Figure 4), PCE concentrations plateau at a concentration of about 60 µg/L, TCE concentrations plateau at about 8 µg/L, *cis*-DCE concentrations at 1.5 µg/L, and VC concentrations at 0.5 µg/L. These simulated concentrations of CEs are not dissimilar to the observed concentrations (Table 2). Especially notable is the lack of measurable VC concentrations at the supply well (Table 2), which is consistent with the simulated low concentrations of VC (Figure 5D). Thus, observed concentrations of CEs are also consistent with the bioavailable fraction of organic carbon (0.15) indicated from the observed and simulated DO concentrations (Figure 5).

The effects of placing a simulated source area in a more distal location near well cluster FSS4 (Figure 3) are shown in Figure 8. The second simulated source area is located further from the public supply well, and the flowpath initially is more anoxic than for the first simulated source area. It would be expected, therefore, that simulated CE concentrations for the second source area would arrive later and at lower concentrations than for the first source area. Inspection of Figure 8 indicates that the CEs arrive at the supply well after about 20 years, 10 years later than for the more proximal simulated source area. Significantly, however, the simulated CE concentrations are not lower. Rather, they are about a factor of 5 higher. The reasons for the discrepancy between the expected and simulated behavior, which will be discussed subsequently, have to do more with hydrologic rather than biochemical factors.

Discussion

The chief utility of the mass balance modeling approach used in this paper is that it makes it possible to quantify how different characteristics of a hydrologic system (Equation 1) affect the vulnerability of public supply wells to CE contamination. It has long been known that the amount and bioavailability of naturally occurring organic carbon is a critical factor controlling the extent of reductive dechlorination, and thus the potential for contaminant transport to wells (Wiedemeier et al. 1999).

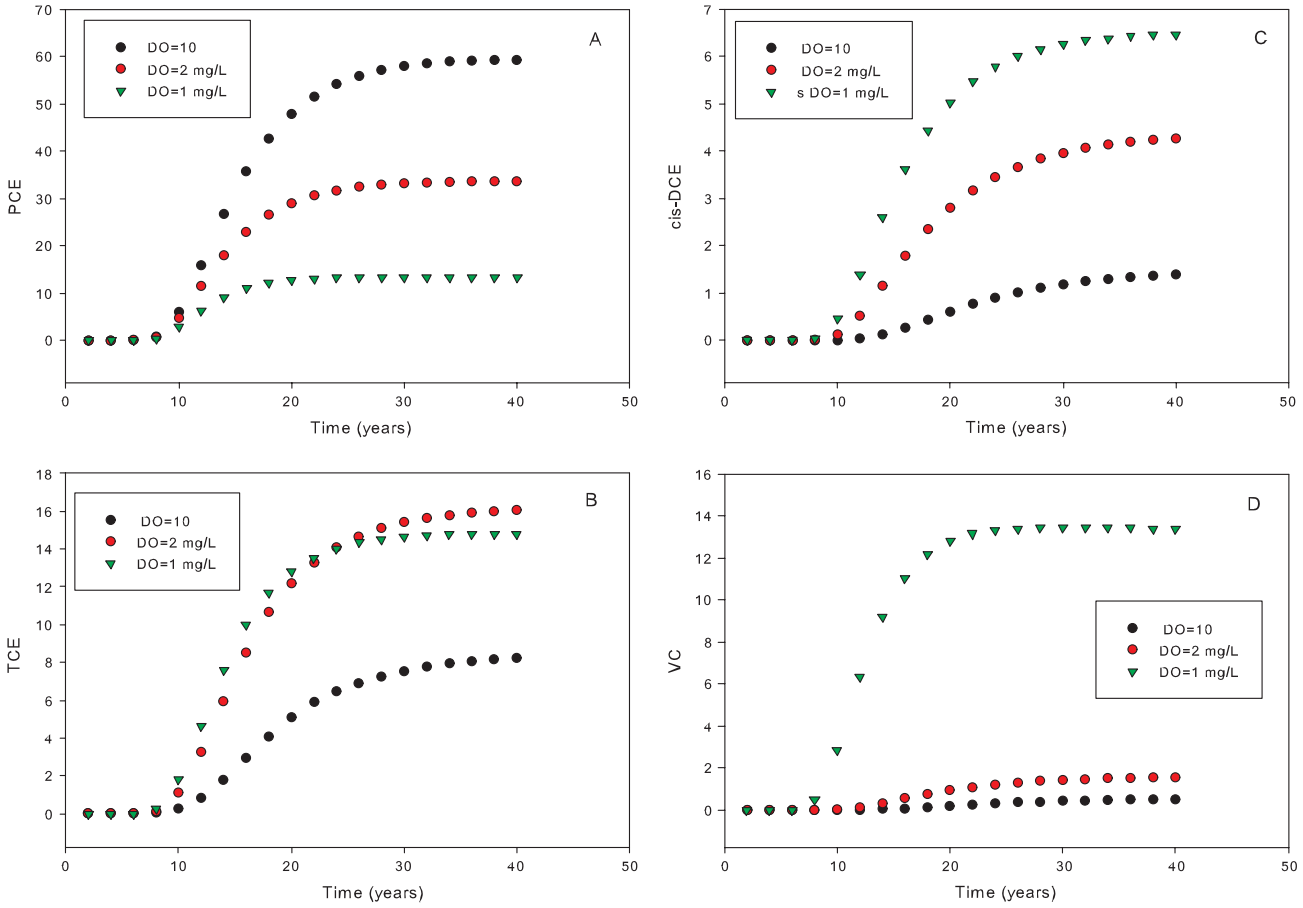

Figure 6. Simulated concentration changes of (A) PCE, (B) TCE, (C) *cis*-DCE, and (D) VC arriving at the public supply well as a function of DO concentrations in aquifer recharge.

It has not, however, previously been possible to examine those effects quantitatively. By directly coupling the availability of electron donors (DOC, POC, and adsorbed organic carbon [AOC]) and EAs (oxygen, CEs, and Fe(III)) in the SEAM3D code, it is possible to examine how they interact and how those interactions affect CE transport to an actual public supply well. In addition, it is possible to examine how variability in aquifer and confining bed properties, recharge rates, and locations of contaminant source areas affect the vulnerability of that public supply well.

The model was initially constrained by comparing observed (Figure 3) and simulated (Figure 4) concentrations of DO in observation wells and the supply well. This procedure suggested that a relatively small fraction (~0.15) of the POC present in the aquifer is actually available to support microbial metabolism. This result, based solely on observed concentrations of DO, is consistent with the observed presence of PCE, TCE, and *cis*-DCE and the observed lack of measurable VC at the supply well (Table 2). Any assumed bioavailable fraction of POC exceeding 0.15 resulted in measurable VC concentrations arriving at the well (Figure 5). Thus, two independent lines of evidence are consistent with a relatively low bioavailable fraction of POC. Considering that the sediments of the Kirkwood-Cohansey aquifer are approximately 20 million years old and that they have functioned as a fresh water aquifer for part of that time, the relatively low fraction of bioavailable organic carbon is unsurprising.

The results of varying the bioavailable fraction of POC from zero to 0.15 suggests that reductive dechlorination has a relatively small effect on the transport of PCE to the public supply well from the first simulated source area (Figure 5). Assuming zero bioavailable POC, simulated PCE concentrations plateau at approximately 80 µg/L. Assuming 0.15 bioavailable POC, however, decreases simulated PCE concentrations to about 60 µg/L. This, in turn, suggests a relatively low impact of reductive dechlorination on concentrations of PCE arriving at the public supply well in this system. This suggestion is consistent with the observed high concentrations of PCE at the public supply well relative to the daughter products TCE and *cis*-DCE (Table 2).

Another potentially important variable affecting CE transport in groundwater systems is the delivery of DO to the aquifer in recharge. The results show that the simulated delivery of CEs to the supply well is highly sensitive to assumed concentrations of DO in recharge water (Figure 6). When recharge is assumed to contain 10 mg/L DO, PCE is delivered to the supply well at relatively high concentrations (Figure 6A). When recharge is assumed to contain only 1 mg/L DO, however, the

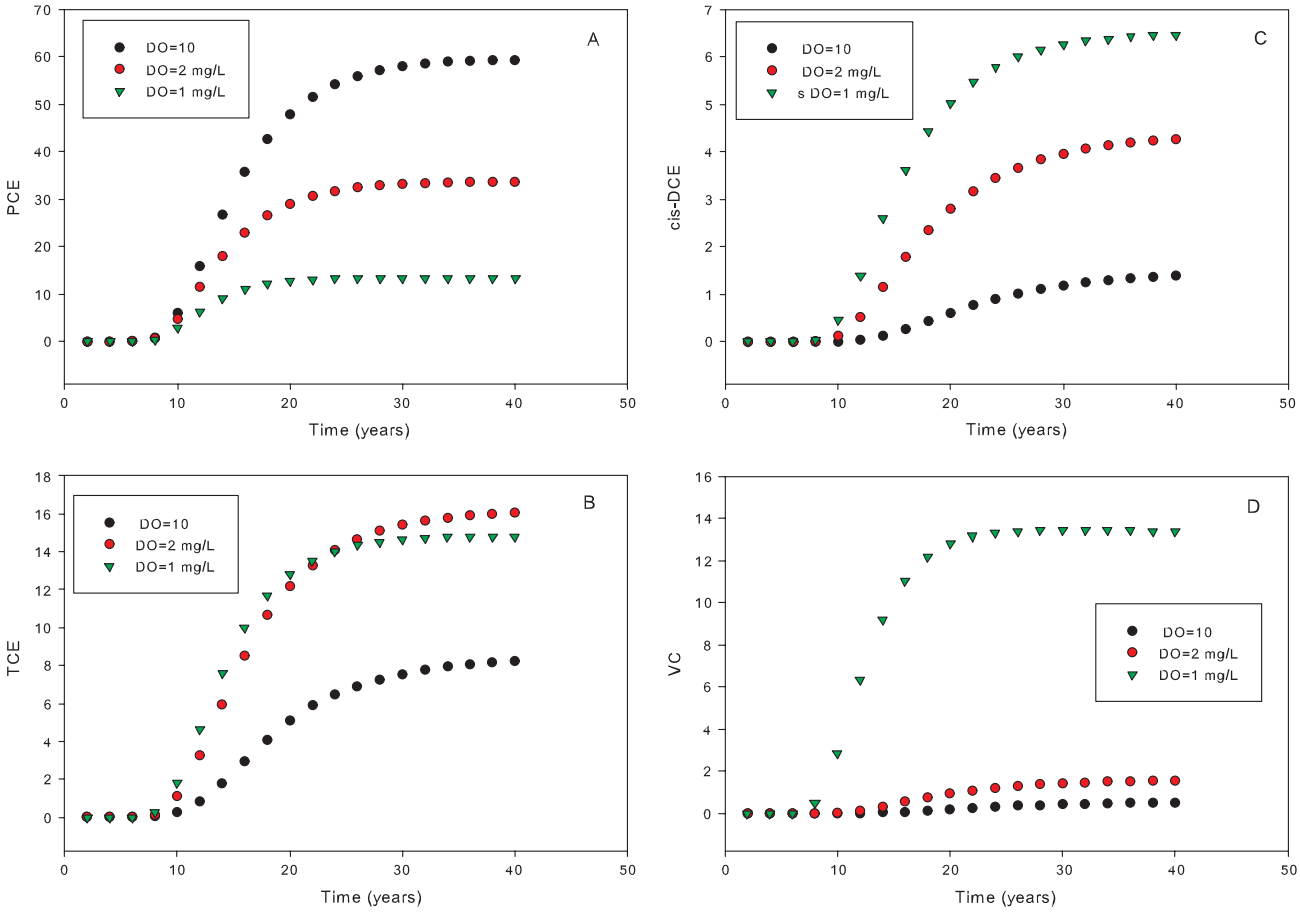

Figure 7. Simulated concentration changes of (A) PCE, (B) TCE, (C) *cis*-DCE, and (D) VC arriving at the public supply well as a function of the concentration of DOC in aquifer recharge.

amount of PCE reaching the supply well declined by about 80% (Figure 6A) with concomitant increases in daughter products (Figure 6B to D). The amount of DO present in aquifer recharge depends on the amount of organic carbon present in soil, the thickness of the unsaturated zone, and rates of recharge and can be expected to vary from system to system. These results suggest that DO concentrations in recharge is an important, and probably underappreciated, factor affecting the vulnerability of wells to CE contamination.

This mass balance approach suggests less sensitivity of CE transport to concentrations of DOC present in recharge (Figure 7). When aquifer recharge assumed to have 0.05 mg/L DOC, which is probably a low value, simulated PCE concentrations plateau at approximately 60 µg/L. Increasing DOC concentrations in recharge to 1.5 mg/L, which is probably a high value for this system (Table 2), only lowers the PCE plateau to about 40 µg/L. One reason for this lack of sensitivity is the interactions of the dissolved, particulate, and adsorbed compartments that store organic carbon. The sequestration of DOC in adsorbed phase acts to buffer DOC concentrations to a narrower range (0.8 to 1.2 mg/L) than is possible for DO (0 to 10 mg/L). This buffering, in turn, can lower the sensitivity of CE transformation to assumed concentrations of DOC in recharge.

The location of potential contaminant source areas relative to public supply wells is an obvious factor in determining vulnerability to contamination. In this particular system, locating a simulated contaminant source area (Figure 2) approximately 700 m upgradient of the supply well leads to breakthrough of PCE in approximately 10 years after release (Figure 5). Locating the simulated source in a more distal area approximately 1000 m from the supply well (Figure 2) increases the time for contaminant breakthrough to about 20 years (Figure 8). Interestingly, however, even though the PCE concentration at both simulated source areas was held constant at 25 mg/L, simulated contaminant concentrations were higher for the more distal source area (Figure 8) than for the more proximal source area (Figure 5). The reason for this is that the flux of recharge from the second source area was significantly higher (39 m^3/d) than for the first source area (14 m^3/d). In addition, the distal source area overlies a low-permeability zone that directs groundwater flowpaths laterally rather than vertically downward (Figure 3). This, in turn, reduces the amount of recharge water entering the anoxic part of the aquifer, which limits CE transformation. This is an illustration of how IS (Equation 1), which includes hydrologic factors such as recharge rates and locations of confining beds, can affect contaminant behavior as much as biogeochemical factors. These model

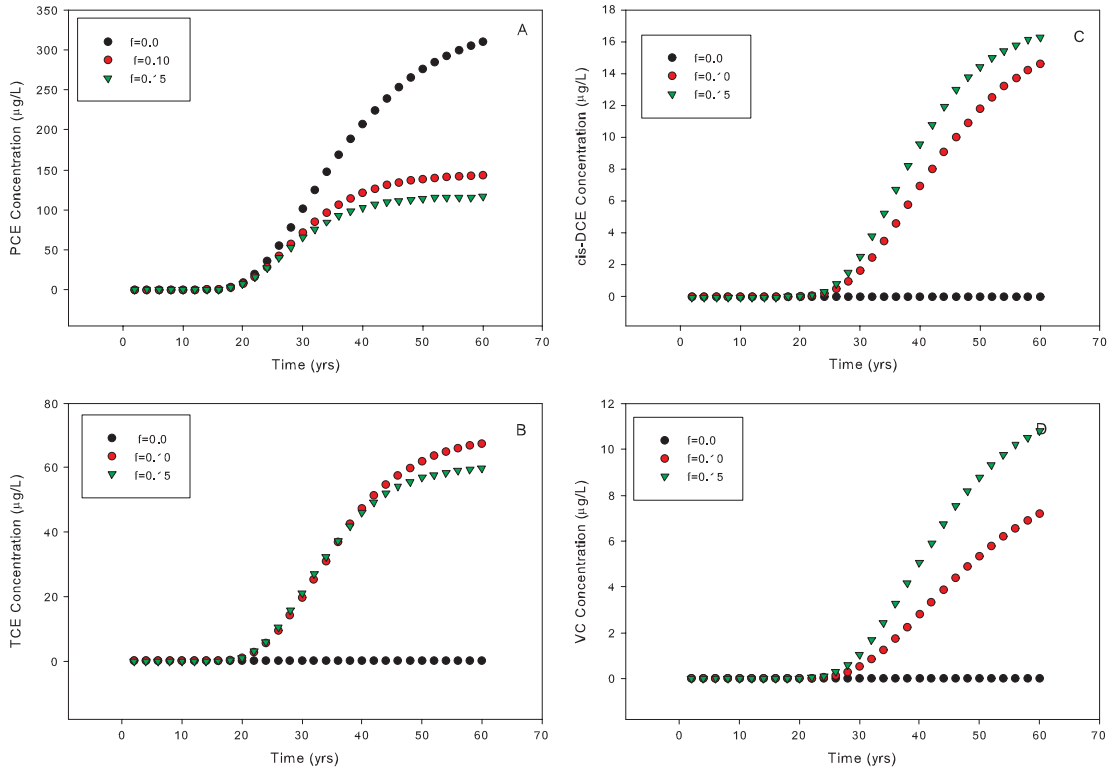

Figure 8. Simulated concentration changes of CEs arriving at the public supply well from a source area overlying the predominantly anoxic portion of the flow system (Figure 3).

simulations also illustrate how IS varies depending on the location of contaminant source areas.

The natural attenuation of CEs in groundwater systems is the result of the sum of advective mixing, hydrodynamic dispersion, sorption, and biodegradation processes. The mass balance approach discussed in this paper makes it possible to quantify the relative effects of hydrodynamic and biodegradation processes. For example, simulated PCE concentrations at the supply well assuming zero percent bioavailable POC plateau at about 80 µg/L for the proximal simulated contaminant source area (Figure 5). Because the simulated source area contributed 25 mg/L PCE, the combined effects of strictly hydrodynamic and sorptive natural attenuation lowered simulated concentrations by a factor of 0.32%. When biological attenuation is added to the hydrodynamic attenuation by assuming 0.15 fraction of bioavailable POC (Figure 5), PCE concentrations plateau at 60 µg/L, or an overall attenuation factor of 0.24%. Clearly in this system, much of the overall simulated natural attenuation results from advective mixing, hydrodynamic dispersion, and sorption rather than biodegradation processes.

Conclusions

The mass balance modeling approach used in this study makes it possible to illustrate the effects that hydrodynamic and biodegradation processes have on the vulnerability of a public supply well to CE contamination. The transport of contaminants to the supply well is highly sensitive to the bioavailability of POC, AOC, and DOC. Similarly, contaminant transport is also highly sensitive to concentrations of DO entering the aquifer with recharge. The modeling results are less sensitive to concentrations of DOC entering the aquifer via recharge. This probably reflects the sequestration of DOC by adsorption processes that serves to buffer DOC concentrations within a relatively small range. Finally, while biodegradation processes are often used synonymously with the term "natural attenuation," the mass balance approach in this study suggests that hydrodynamic processes such as advective mixing and dispersion account for a much greater percentage of overall attenuation than biodegradation processes in this aquifer system.

Acknowledgments

This research was supported by the National Water Quality Assessment (NAWQA) and Toxic Substances Hydrology Programs of the U.S. Geological Survey. Mark Widdowson should be contacted concerning the availability of SEAM3D.

References

Aiken, G. 1989. Organic matter in ground water. U.S. Geological Survey Open File Report 02–89, 7 p. Reston, Virginia: USGS.

Bradley, P.M. 2003. History and ecology of chloroethene biodegradation: A review. *Biodegradation Journal* 7, no. 2: 81–109.

Cauller, S.J., and G.B. Carleton. 2005. Hydrogeology and simulated effects of ground-water withdrawals, Kirkwood-Cohansey aquifer system, Upper Maurice River Basin area, New Jersey. U.S. Geological Survey Scientific Investigations Report 2005–5258, 48 p. Reston, Virginia: USGS.

Chapelle, F.H., L.K. Thomas, P.M. Bradley, H.V. Rectanus, and M.A. Widdowson. 2012. Threshold amounts of organic carbon needed to initiate reductive dechlorination in groundwater systems. *Remediation Journal* 22, no. 3: 19–27.

Chapelle, F.H., J. Novak, J. Parker, B.G. Campbell, and M.A. Widdowson. 2007. A framework for assessing the sustainability of monitored natural attenuation. U.S. Geological Survey Circular 1303, 35 p. Reston, Virginia: USGS.

Davis, J.A. 1982. Adsorption of natural dissolved organic matter at the oxide/water interface. *Geochimica et Cosmochimica Acta* 46: 2381–2393.

Feinstein, D.T., and M.A. Thomas. 2008. Hypothetical modeling of redox conditions within a complex ground-water flow field in a glacial setting. U.S. Geological Survey Scientific Investigations Report 2008–5066, 28 p. Reston, Virginia: USGS.

Findlay, S., and W.V. Sobczak. 1996. Variability in removal of dissolved organic carbon in hyporheic sediments. *Journal of the North American Benthological Society* 15, no. 1: 35–41.

Focazio, M.F., T.E. Reilly, M.G. Rupert, and D.R. Delsel. 2002. Assessing ground-water vulnerability to contamination: Providing scientifically defensible information for decision makers. U.S. Geological Survey Circular 1224. Reston, Virginia: USGS.

Frind, E.O., J.W. Molson, and D.L. Rudolph. 2006. Well vulnerability: A quantitative approach for source water protection. *Ground Water* 44, no. 5: 732–742.

Gu, B., J. Schmitt, Z. Chen, L. Liang, and J.F. McCarthy. 1995. Adsorption and desorption of different organic matter fractions on iron oxide. *Geochimica et Cosmochimica Acta* 59, no. 2: 219–229.

Harbaugh, A.W. 2005. MODFLOW-2005, the U.S. Geological Survey modular ground-water model—The ground-water flow process. U.S. Geological Survey Techniques and Methods 6-A16. Reston, Virginia: USGS.

Harbaugh, A.W., and M.G. McDonald. 1996. User's documentation for MODFLOW-96, and update to the U.S. Geological Survey modular finite-difference ground-water flow model. U.S. Geological Survey Open-File Report 96–485, 56 p. Reston, Virginia: USGS.

Jardine, P.M., M.A. Mayes, P.J. Mulholland, P.J. Hanson, J.R. Tarver, R.J. Luxmoore, J.F. McCarthy, and G.V. Wilson. 2004. Vadose zone flow and transport of dissolved organic carbon at multiple scales in humid regimes. *Vadose Zone Journal* 5: 140–152.

Kahle, M., M. Kleber, and R. Jahn. 2004. Retention of dissolved organic matter by phyllosilicate and soil clay fractions in relation to mineral properties. *Organic Geochemistry* 35: 269–276.

Kalbitz, K., S. Solinger, J.H. Park, B. Michalzik, and B. Matzner. 2000. Controls on the dynamics of dissolved organic matter in soils: A review. *Soil Science* 165, no. 4: 277–304.

Kauffman, L.J., A.L. Baehr, M.A. Ayers, and P.E. Stackelberg. 2001. Effects of land use and travel time on the distribution of nitrate in the Kirkwood-Cohansey aquifer system in southern New Jersey. U.S. Geological Survey Water-Resources Investigations Report 01–4117, 49 p. Reston, Virginia: USGS.

Leenheer, J.A. 1974. Occurrence of dissolved organic carbon in selected groundwater samples in the United States. *U.S. Geological Survey Journal of Research* 2: 361–369.

Lilienfein, J., R.G. Qualls, S.M. Uselman, and S.D. Bridgham. 2004. Adsorption of dissolved organic carbon and nitrogen in soils of a weathering chronosequence. *Soil Science* 68: 292–305.

McMahon, P.B., and F.H. Chapelle. 2008. Redox processes and the water quality of selected principal aquifer systems. *Ground Water* 46, no. 2: 259–285.

McMahon, P.B., and F.H. Chapelle. 1991. Microbial organic-acid production in aquitard sediments and its role in aquifer geochemistry. *Nature* 349: 233–235.

McMahon, P.B., D.F. Williams, and J.T. Morris. 1990. Production and carbon isotopic composition of bacterial CO_2 in deep Coastal Plain sediments of South Carolina. *Ground Water* 28, no. 5: 693–702.

Oren, A., and B. Chefetz. 2012. Sorptive and desorptive fractionation of dissolved organic matter by mineral soil matrices. *Journal of Environmental Quality* 41: 526–533.

Owens, J.P., and J.P. Minard. 1979. Upper Cenozoic sediments of the lower Delaware Valley and the northern Delmarva Peninsula, New Jersey, Pennsylvania, Delaware, and Maryland. U.S. Geological Survey Professional Paper 1077-D, 47 p. Reston, Virginia: USGS.

Rectanus, H.V., M.A. Widdowson, F.H. Chapelle, C.A. Kelly, and J.T. Novak. 2007. Investigation of reductive dechlorination supported by natural organic carbon. *Ground Water Monitoring and Remediation* 27, no. 4: 53–62.

Thomas, L.K., M.A. Widdowson, F.H. Chapelle, J.T. Novak, J.E. Boncal, and C.A. Lebrón. 2013. Distribution of potentially bioavailable natural organic carbon in aquifer sediments at a chloroethene-contaminated site. *Journal of Environmental Engineering* 139, no. 1: 54–60.

Thurman, E.M. 1985. *Organic Geochemistry of Natural Waters*, 497. Dordrecht, The Netherlands: Martinus Nijhoff/DR W. Junk Publishers.

U.S. EPA. (1998). Technical protocol for evaluating monitored natural attenuation of chlorinated solvents in ground water, EPA/600/R-98/128. Washington, DC: United States Environmental Protection Agency.

Waddill, D.W., and M.A. Widdowson. 2000. SEAM3D: A numerical model for three-dimensional solute transport and sequential electron acceptor-based bioremediation in groundwater, ERDC/EL TR-00-X, 89 p. Vicksburg, Mississippi: U.S. Army Engineer Research and Development Center.

Waddill, D.W., and M.A. Widdowson. 1998. A three-dimensional model for subsurface transport and biodegradation. *Journal of Environmental Engineering* 124, no. 4: 336–344.

Wiedemeier, T.H., H.S. Rifai, C.J. Newell, and J.T. Wilson. 1999. *Natural Attenuation of Fuels and Chlorinated Solvents in the Subsurface*. New York: Wiley.

Widdowson, M.A. 2004. Modeling natural attenuation of chlorinated ethenes under spatially-varying redox conditions. *Biodegradation* 15: 435–451.

Zogorski, J.S., J.M. Carter, T. Ivahnenko, W.W. Lapham, M.J. Moran, B.L. Rowe, P.J. Squillace, and P.L. Toccalino. 2006. Volatile organic compounds in the nation's ground water and drinking-water supply wells. U.S. Geological Survey Circular 1292, 101 p. Reston, Virginia: USGS.